Reaction-bonded boron carbide for lightweight armor:

The interrelationship between processing, microstructure, and mechanical properties

Credit: Paxis

A BorLite reaction-bonded boron carbide armor plate, manufactured by Paxis Ltd. (Savion, Israel), after impact with 7.62X63 AP M2 projectiles.

By Shmuel Hayun

With adequate understanding of processing parameters and resulting material properties, reaction bonding offers a relatively inexpensive alternative fabrication method for lightweight ceramic armor.

Since the dawn of history, weapons and armor have been in a life-and-death struggle. During the last three decades of the 20th century, a variety of ceramics, including aluminum nitride (AlN), aluminum oxide (Al_2O_3), boron carbide (B_4C), silicon carbide (SiC), titanium diboride (TiB_2), tungsten carbide (WC), and zirconium oxide (ZrO_2), were investigated as armor materials.

Light ceramics particularly are attractive for personnel as well as land and airborne vehicle protection. The most commonly used ceramics are Al_2O_3, SiC, and B_4C. Al_2O_3 is the most economical alternative, but its final protection solutions are heavier, because Al_2O_3 has the highest density and lowest ballistic efficiency of the three light ceramics. B_4C is the hardest ceramic, but it undergoes an amorphization process at high impact pressures (such as with WC-cored bullets), which weakens the armor. Although SiC has no amorphization issues, its higher density (3.2 g/cm^3) compared with B_4C (2.52 g/cm^3) limits its use.

We must consider some other points when choosing an adequate armor material. For instance, low porosity in the ceramic tile generally results in better ballistic performance. Moreover, smaller grain sizes increase ballistic performance. In addition, ease of fabrication and cost are of paramount importance in considering a particular material for armor applications. Full density of B_4C or SiC is a prerequisite for achieving acceptable ballistic resistance, but can be attained only by hot-pressing fine powder (<2 μm) in the presence of sintering additives at relatively high temperatures (>2,473 K). Further, production method strongly affects properties of the ceramic: hot-pressing tiles often results in a harder ceramic, which is optimal against a single hit, whereas reaction-bonding tiles provide better multihit performance. However, there is no

Capsule summary

THE POTENTIAL

Reaction-bonding fabrication methods offer a low-cost route to produce composites with effective ballistic impact resistance, generating materials with great potential for lightweight armor applications.

THE CAVEAT

Despite the potential of reaction-bonded materials for armor applications, processing variables in reaction-bonding techniques can significantly reduce mechanical properties of resulting composites.

THE SOLUTION

Better understanding of the effect of processing parameters on the microstructure of infiltrated composites, their static and dynamic mechanical properties, and microstructure–property relationships can help develop more efficient reaction-bonded boron carbide for lightweight armor applications.

clear correlation between quasi-static and/or dynamic mechanical properties and the ballistic behavior of ceramics. Nonetheless, some parameters, such as hardness, fracture toughness, and elastic modulus, are expected to have an influence.

Elevated hardness values are, by common consensus, crucially important for good ballistic resistance, because a material with sufficiently high hardness deforms or fragments a projectile upon impact.[1] Moreover, ceramic fragments may continually abrade the projectile during the rest of the penetration process.[2] It is, however, unclear if harder is always better, because one of the main failure modes of thin ceramic tiles is related to fracture from tensile stresses, which higher hardness does not improve.

Competition between high performance of carbide ceramics and the high cost of conventional fabrication methods led to the development of relatively inexpensive alternative fabrication methods capable of providing adequate mechanical properties. One approach is based on the reaction-bonding technique. According to this approach, ceramic powder (SiC, B_4C, or B_4C–SiC mixture) is mixed with free carbon, compacted, and subsequently infiltrated with molten metal (e.g., silicon or aluminum alloys). Molten metal reacts with free carbon and with carbon that originates in B_4C to form a ceramic composite. The resulting composite has high cohesive strength and elevated hardness values and is an effective ballistic impact-resistant material. Several variants of reaction-bonding processes, as well as the properties of final composites, are described in scientific journals and in patents.

One crucial drawback associated with reaction-bonded composites, however, is the fraction of the residual metal/alloy that significantly reduces the composite's mechanical properties. This fraction strongly depends on initial porosity of the preforms and on the fraction of additional free carbon. Several approaches can reduce initial preform porosity, including partial sintering, use of multimodal powder mixtures, addition of elements that react with the alloy/metal to form stable phases, and addition of elements (e.g., titanium or iron) or compounds (e.g., TiC) that react with B_4C and release additional free carbon.

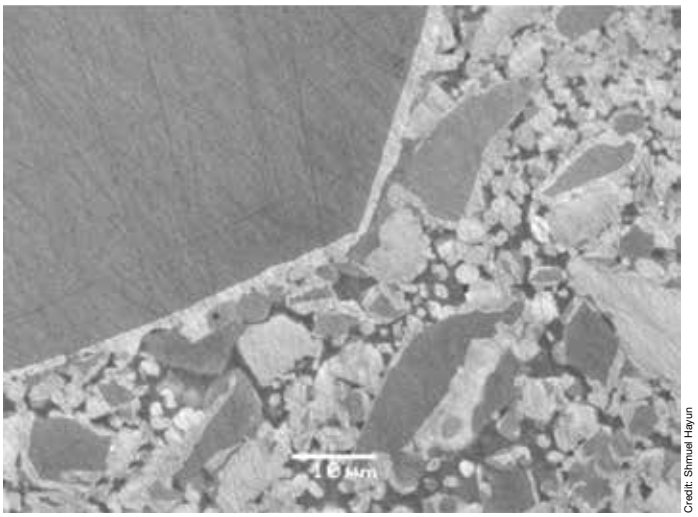

Credit: Shmuel Hayun

Figure 1. Scanning electron micrograph of RBSC composite. The new SiC layer (white color) precipitates on initial SiC particles (darker color).

Thus, knowledge of the effect of processing parameters on the microstructure of infiltrated composites, their static and dynamic mechanical properties, and microstructure–property relationships is necessary to understand and develop more efficient armor.

Processing of reaction-bonded composites

Reaction bonding is a special case of reaction-forming processes that represent an important alternative to conventional sintering processes, such as solid-state sintering, liquid-phase sintering, and hot pressing. For polycrystalline ceramics fabricated by processes involving chemical reactions, consolidation between constitutive particles occurs by formation of new phases rather than by a neck-growth mechanism induced by relatively weak surface energy forces. In general, these processes have the advantage of reducing working temperature, shaping materials in potentially complex and large near-net shapes, and reducing or even canceling postconsolidation machining. All these make the reaction-forming process an obvious direct cost–benefit method. The most important and widely used reaction-forming processes are based on reactions between a porous solid and an infiltrating liquid phase.

Reaction-bonded silicon carbide (RBSC) composites

The reaction-bonding approach was first suggested and developed in the 1950s for SiC.[3] According to this approach, a porous body (preform) consisting of the ceramic phase and free carbon is infiltrated with liquid silicon, which reacts with the carbon to form a secondary SiC phase. The resulting microstructure (Figure 1) consists of original SiC particles surrounded by a secondary SiC phase and 5–15 vol% of residual silicon.[4] Pre-existing, primary SiC particles are bonded by the newly formed SiC phase. A recent spin-off that uses diamond as a carbon source shows huge potential—the new composites show elevated stiffness, hardness, and thermal conductivity values.

The microstructure and mechanical properties of RBSC have been thoroughly investigated. Previous studies established the effect of compacted preform properties (porosity, pore size and distribution, fraction of free carbon, and carbon source) and processing parameters (temperature and duration of the infiltration procedure as well as cooling regime) on the microstructure of infiltrated composites and their mechanical properties.[5]

RBSC materials display high mechanical properties, including hardness (15–25 GPa), Young's modulus (320–400 GPa), flexural strength (100–400 MPa), and fracture toughness (~3.9 MPa·m$^{1/2}$).[6] Two main factors determine mechanical properties of an RBSC:

- Fraction of residual silicon, the properties of which are significantly lower than those of the SiC phase; and
- Structure and strength of the interfaces between RBSC phases.

The first factor is straightforward—we can reduce the fraction of residual silicon by adding reactive elements to the silicon melt. These elements react with residual liquid silicon to form silicide phases. The second factor is more complex and is discussed widely in the literature. Reported results regarding the nature of Si/SiC and α-SiC/β-SiC interfaces are summarized in a review by Ness and Page,[7] who conclude that occasional misfit dislocations and steps are formed at Si/SiC interfaces. These observations are in good agreement with the results of Naylor and Page,[8] who show that the Si/SiC interface is mechanically weak and provides a preferential path for fracture under indentation. Interfaces between β-SiC and α-SiC are semicoherent, and it is suggested that SiC/SiC α/α, α/β, β/α and β/β) grain boundaries are strongly bonded by a thin layer (~1 nm) of amorphous SiC.

Reaction-bonded boron carbide (RBBC) composites

In 1973, Taylor and Palicke[9] submitted a patent on "Dense carbide composite for armor and abrasives." In this patent and other papers, Taylor and Palicke touch upon several key issues of the process that recurrently is referred to in subsequent patents. The authors fabricated dense carbide composites using the same technique for RBSC, but, instead of SiC, they used B_4C. They discuss issues, including the source of the carbon that is meant to react with molten silicon (which may be a free-carbon addition), a carbon-based binder (which provides minimal self-supporting strength to the green body), or B_4C itself (which releases carbon when in contact with molten silicon). Taylor and Palicke also discuss the importance of B_4C particle-size distribution and its effect on efficient volume filling. The authors argue that at least 12 vol% of residual silicon is necessary to achieve good fabrication yields (i.e., composites without cracks). This requirement puts a major drawback on RBBC, similar to RBSC, where residual silicon creates soft spots that detract from overall ballistic efficiency of the product. Since then, the research has expanded to overcome this obstacle and to reduce the amount of residual silicon in RBSC.

Table 1. Technological parameters of specimen fabrication

Specimen	Initial particle size (μm)	Partial sintering, 30 min	Carbon addition	Alloying elements	Porosity of preform (vol%)
RB	1, 5, 100	No	No	No	30, 45
RBM	Multimodal powder mixtures†	No	No	No	25
RI	1, 5	2,173–2,373 K	No	No	20, 30, 40
RIC	1, 5	2,173–2,373 K	Yes	No	20, 30, 40
RITC‡	1, 5	2,343–2,403 K	No	TiC	20, 30, 40
RIFE§	5	2,273 K	No	Fe	30

†Powder mixture consists of 60, 15, and 25 parts of particles with average sizes of 106, 13, and 1 μm.

‡RITC is reaction infiltration of partly sintered B_4C–TiC body infiltrated with carbon.

§RIFE is reaction infiltration of partly sintered B_4C–Fe body infiltrated with silicon

Fabrication approaches for RBBC composites

The fraction of residual silicon strongly depends on initial porosity of the preforms and on initial fraction and distribution of free carbon within a compacted body. To reduce initial porosity of the preforms, we can either partly sinter B_4C compacts to a desired porosity or use a mixture of optimally distributed B_4C powders of various average particle sizes.

At early stages of our work, we realized that use of resins as a source of free carbon should be avoided, because toxic gases are released during pyrolysis. Thus, we used several alternative methods, including pyrolysis of commercial sugar after drying a 50:50 water solution and addition of carbon content (TiC) or carbon release elements (iron) to B_4C, where the reaction between these compounds releases free carbon. Technological parameters for specimen fabrication are presented in Table I.

Microstructure and phase composition of B_4C composites

Studies establish the microstructure and phase composition of silicon-infiltrated B_4C composites fabricated via various approaches. The following phase compositions were studied:

- Reaction-bonded (RB, green B_4C body infiltrated with silicon);
- Reaction-bonded multimodal (RBM, green B_4C body made of multimodal particles infiltrated with silicon;
- Reaction-infiltrated (RI, partly sintered body infiltrated with silicon); and
- Reaction-infiltrated with added carbon (RIC, partly sintered body with added free carbon and infiltrated with silicon).

These materials consist of four phases: original B_4C particles; ternary $B_{12}(B,C,Si)_3$ compound; β-SiC; and residual silicon (Figure 2). The reaction between molten silicon and B_4C particles results in core–rim structure formation and a β-SiC phase of single platelike particles.

Aghajanian et al.[10] stress that the reaction of molten silicon with B_4C has a deleterious effect and suggest the use of boron as an alloying element to silicon to curtail its interaction with the ceramic matrix. However, thermodynamic analysis and experimental results show that formation of the silicon-containing B_4C compound $B_{12}(B,C,Si)_3$ during the RBBC process is independent of the fabrication approach and always occurs in the B-C-Si system. Results from

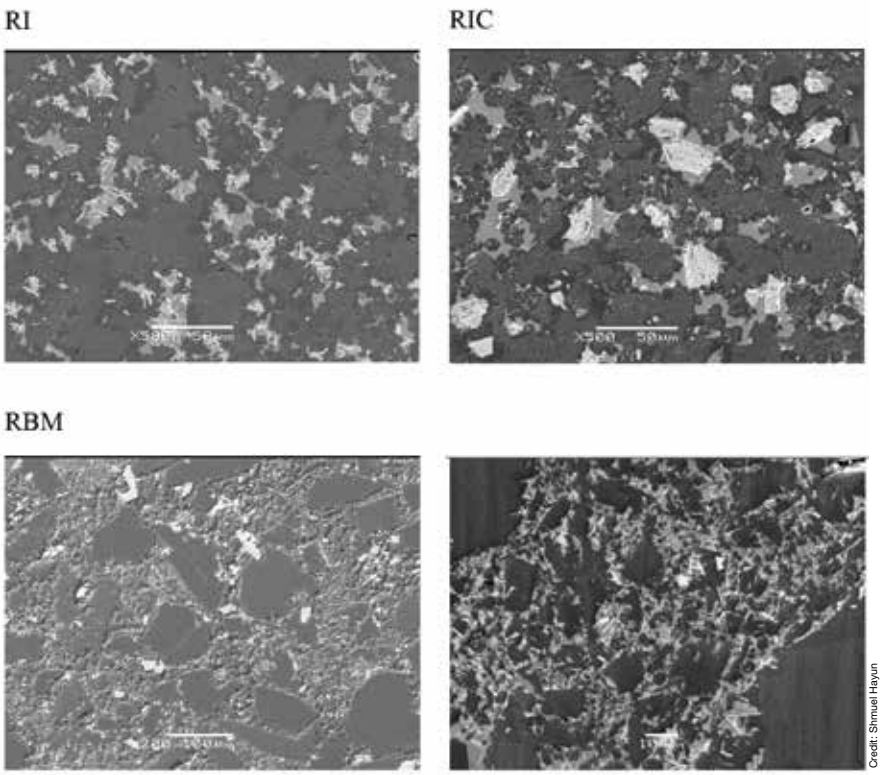

Credit: Shmuel Hayun

Figure 2. Scanning electron micrographs of bulk regions in RI, RIC, and RBM composites. In RBM composite, left image shows microstructure after removal of residual silicon; right image shows enlarged area between two large B_4C grains.

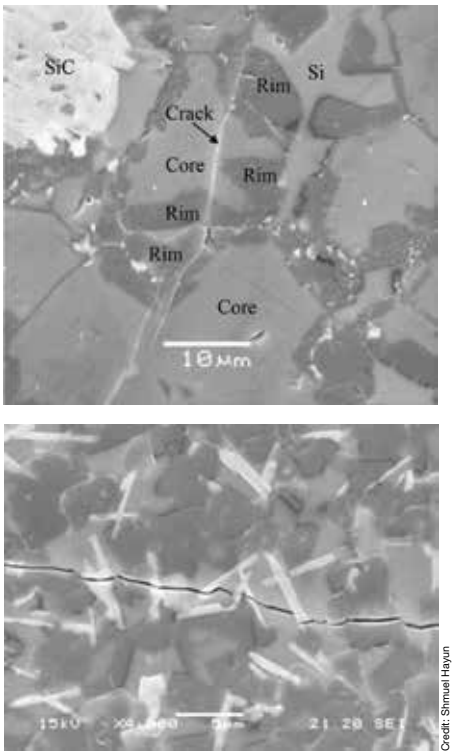

Credit: Shmuel Hayun

Figure 3. Crack propagation path in the composite underlines strength of the boundary between the B_4C particle core and adjacent rim. Moreover, interaction with SiC plates causes multiple crack deflections.

nanoindentation experiments show that average hardness and Young's modulus values of the $B_{12}(B,C,Si)_3$ phase (H_V = 46.1 + 4.2 GPa and E = 474 + 34 GPa, respectively) are slightly higher than those of the initial B_4C phase (H_V = 42.0 + 3.3 GPa and E = 460 + 23 GPa).[11] In addition, inspection of a crack propagation path indicates that the boundary between core and rim regions is relatively strong and does not deflect the propagating crack (Figure 3). Thus, the newly formed $B_{12}(B,C,Si)_3$ phase does not reduce mechanical properties of the composite.

The mechanism of core–rim structure formation is attributed to the dissolution precipitation process, which is well accounted for by thermodynamic analysis of the B-C-Si system.[12] Because B_4C is a covalently bonded solid, its components diffuse at an extremely low rate, and, therefore, it dissolves congruently (i.e., with no compositional changes). Boron concentration in the melt as a result of congruent dissolution is 8.0 at.% of boron. At the same time, boron content in the melt, which is in equilibrium with SiC and the ternary $B_{12}(B,C,Si)_3$ phase, is ~6.6 at.%. Thus, congruent dissolution of B_4C provides the required oversaturation for ternary carbide formation, and precipitation of the $B_{12}(B,C,Si)_3$ phase establishes overall equilibrium conditions in the system. Precipitation of the ternary carbide phase takes place at the interface of original B_4C particles and leads to formation of rim regions. The dissolution–precipitation process continues as long as the liquid is in contact with original B_4C particles.

The amount of various phases within RBBC composites is strongly affected by two factors, neither of which is free-carbon addition (Table 2). The first and obvious factor is initial porosity of the preforms, which determines amount of residual silicon and

Table 2. Average phase distribution in carbon-free and carbon-containing composites

Material	Initial porosity	B_4C (vol%)	SiC (vol%)	Silicon (vol%)	Material	Initial porosity	Free carbon (vol%)	B_4C (vol%)†	SiC (vol%)	Silicon (vol%)
RI(P_1)‡	20	80 ± 3	13 ± 1	7 ± 1	RIC(P_1)‡	20	3 ± 0.5	80 ± 3	12 ± 1	8 ± 1
	30	70 ± 3	17 ± 1	13 ± 1		30	3 ± 0.5	70 ± 3	17 ± 1	13 ± 1
	40	60 ± 3	20 ± 1	20 ± 1		40	5 ± 0.5	60 ± 3	24 ± 1	16 ± 1
RI(P_5)‡	20	80 ± 3	8 ± 1	12 ± 1	RIC(P_5)‡	20	3 ± 0.5	80 ± 3	8 ± 1	12 ± 1
	30	70 ± 3	10 ± 1	20 ± 1		30	4 ±0.5	70 ± 3	9 ± 1	21 ± 1
	40	60 ± 3	12 ± 1	28 ± 1		40	6 ± 0.5	60 ± 3	10 ± 1	30 ± 1
RBM(P_75)‡	25	84 ± 2	6 ± 1	10 ± 1	RB(P_5)‡	30		69 ± 2	11 ± 1	20 ± 1

†Boron carbide: $B_4C + B_{12}(B,C,Si)_3$.

‡P_*X* is initial B4C average particle size (mm).

the newly formed SiC phase. The second factor is related to initial particle size of B_4C. Amount of SiC in the final composite decreases with increasing initial particle size for a given process time. This feature is related to available B_4C surface for interaction with molten silicon, which is significantly higher for fine initial B_4C particles.

In the case of free-carbon addition to the green body prior to infiltration, amount of SiC that forms also strongly depends on initial porosity, with little influence from carbon addition. This "strange" fact may be related to thermodynamic equilibrium in the Si-B-C system for a given temperature. Free carbon "eats" some of the infiltrated silicon and leaves less silicon to interact with B_4C, resulting in less SiC formation from the Si–B_4C interaction. Data in Table 2 show that the total amount of SiC in RIC is very close to carbon-free samples (RI and RB), with similar particle sizes and initial porosity.

Another microstructural feature in this system that strongly depends on processing parameter is morphology of the newly formed SiC phase. In composites fabricated with free-carbon addition, SiC particles display a polygonal shape. For composites in which initial B_4C is the sole source of carbon, the SiC phase displays a platelike morphology. According to transmission electron microscopy analysis, the β-SiC phase always precipitates as single platelike particles from the silicon melt, preferably with the $\{111\}_\beta$ habit plane at the first stage. Available amount of carbon for SiC formation during the process stands behind the different morphology.

Pampuch et al.[13] and Ness and Page[14] discuss the mechanism of SiC formation in RBSC-based composites. At initial stages of the interaction, carbon is suggested to dissolve in the silicon melt, similar to a system without SiC particles.[15] This dissolution provides a gradient of carbon concentrations between the dissolution site and original SiC particles. Carbon diffuses to the surface of SiC particles, and newly formed SiC heterogeneously precipitates. These processes form the specific microstructure of RBSC composites (Figure 1). Moreover, Ness and Page[14] point out that formation of the β-SiC phase in RBSC composites starts as fingerlike particles, which transform to platelike shapes that then broaden to polygonal shapes.

In RBBC composites fabricated in the presence of free carbon, two carbon sources are available for SiC formation. Moreover, solubility of carbon in the silicon melt at equilibrium with SiC is extremely low and does not depend on carbon source. Nevertheless, in the vicinity of B_4C particles, conditions for SiC formation are different from those for free-carbon particles. Carbon and boron dissolve from B_4C particles into the silicon melt, and SiC and $B_{12}(B,C,Si)_3$ phases precipitate. The ternary carbide phase precipitates at the surface of original B_4C particles via a semicoherent interface and competes with SiC for carbon atoms.

SiC particles are nucleated within the melt only up to the stage at which dissolution of B_4C in the molten silicon

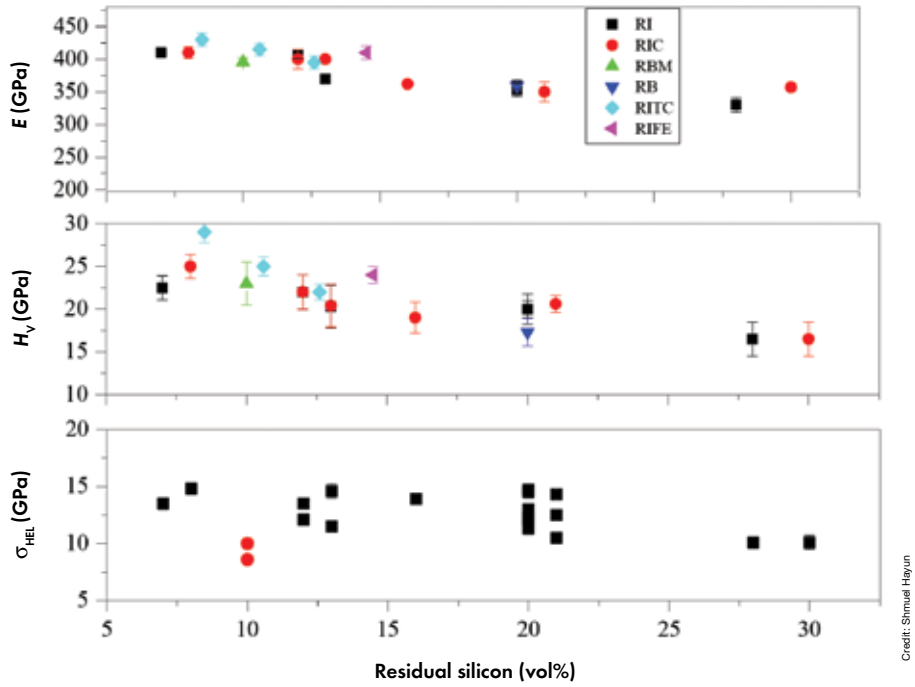

Figure 4. Elastic modulus, Vickers hardness, and σ_{HEL} of composites as a function of residual silicon.

increases the concentration of boron to its solubility limit. At this point, the ternary $B_{12}(B,C,Si)_3$ compound begins to precipitate at the carbide–melt interface and forms rim regions. Further growth of SiC nuclei is controlled by the available amount of carbon, which is significantly lower than in the vicinity of free-carbon particles. These particles are commonly a product of pyrolysis of carbon-rich organics and have a spongelike structure with extremely high specific surface area. Thus, many SiC nuclei form at the carbon–liquid interface. These nuclei begin to grow as plates, which coalesce and form SiC/SiC grain boundaries within polygonal SiC particles by a mechanism similar to that for RBSC composites.

Thus, carbon availability is a key factor for morphology of the β-SiC phase. If B_4C is the only carbon source, the amount of carbon is limited, and β-SiC particles have a platelike shape. If free carbon is present in the green body and other phases do not compete with SiC, most β-SiC particles have a polygonal shape.

Effect of microstructural features on static and dynamic mechanical properties

Elastic modulus (Young's modulus, in particular) and hardness values of composites decrease with increasing fraction of residual silicon (Figure 4). Hardness values refer to average hardness of the composite and reflect contribution of various phases, with a wide range of specific hardness values (see Hayun et al., 2009).[16] These properties depend solely on the residual silicon fraction. Initial size of B_4C particles, element attrition, and morphology of SiC inclusions do not affect elastic modulus and hardness of the composites.

Dynamic mechanical properties (i.e., Hugoniot elastic limit (HEL))[17] show similar tendency for samples with similar particles sizes (~1–5 μm) (Figure 4). The σ_{HEL} values obtained with RBM composites—characterized by low content of residual silicon (~10 vol%), but relatively large average initial particle sizes (~70 μm)—lie far apart from the other current HEL data.

Although elastic modulus and hardness are almost independent from initial size of B_4C particles, HEL, dynamic and static flexural strength, dynamic tensile (spall) strength, and fracture toughness are strongly affected. For example, in composites made from B_4C with particles size of ~1–5 μm without carbon addition (RI and RB specimens), spall strength drops to zero at impact stresses in the range of 8–9 GPa. In RIC specimens (larger SiC particles compared with RI and RB), loss of strength takes place significantly earlier, at impact stresses of 6–7 GPa. In RBM composites, spall strength decreases to zero even under weak impact conditions (>1 GPa), and specimens seem to completely disintegrate under weak compression. HEL decreases from 15 GPa for 1-μm samples to 10 GPa when the initial B_4C particle size is 75 μm. Flexural strength and fracture toughness also decease with increasing average particle (grain) sizes.

Moreover, static flexural strength and fracture toughness show strong dependency on specific SiC morphology (Figure 5). Flexural strength of composites with added carbon (RIC and TIC) is significantly lower than that of RI and RB composites, where B_4C is a sole source of carbon for SiC formation and SiC inclusions have a platelike morphology. Relatively low values of

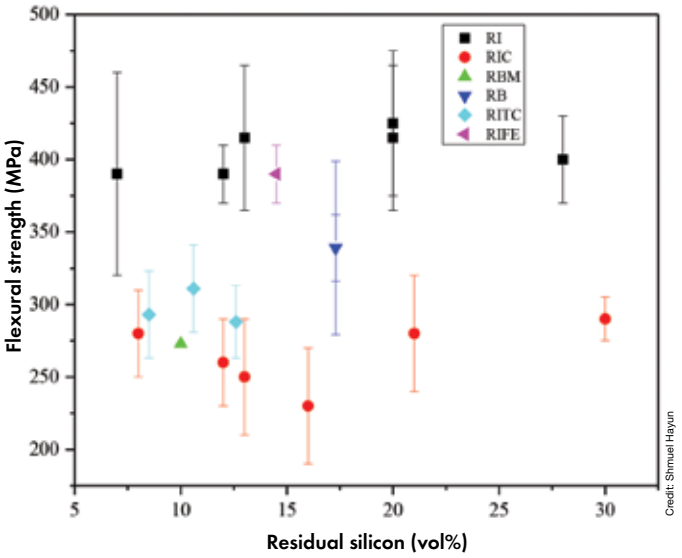

Figure 5. Flexural strength of composites as a function of fraction of residual silicon.

flexural strength for RBM specimens (also fabricated without free-carbon addition) originate from large particle sizes. A similar tendency is observed for fracture toughness of the composites. Values of fracture toughness for RI and RB composites, fabricated in the absence of free carbon using preforms with ~30 vol% porosity, are K_{IC} = 3.62 ± 0.16 MPa·m$^{1/2}$ and K_{IC} = 4.11 ± 0.36, respectively. Fracture toughness of RIC composites fabricated with added carbon is much lower, at K_{IC} = 2.85 ± 0.35 MPa·m$^{1/2}$. Elevated fracture toughness values of RBM specimens

(K_{1C} = 3.25 MPa·m$^{1/2}$) indicate that SiC morphology has a major effect on K_{1C}, whereas influence of initial size of B_4C particles on K_{1C} is minor.

The strengthening effect of platelike SiC particles on ceramic composites based on SiC is well-known.[18] Presence of SiC particles with a platelike morphology affects crack propagation through B_4C-based composites (Figure 3). As noted above, the volume fraction of SiC particles in composites fabricated from preforms with a given porosity does not depend on carbon source. Moreover, polygonal SiC particles are significantly coarser than platelike particles. These features stand behind the increased per unit volume of particles with a platelike morphology. An increase of finer particles is associated with more boundaries that are to be crossed by propagating cracks, thereby decreasing crack energy.

Up to this point, the discussion has centered on how amount of residual silicon, SiC morphology, and average grain size affect mechanical properties. An additional processing parameter with a strong impact on production cost is a preliminary sintering stage for producing a strong skeleton ceramic body, which is thought to reduce the amount of silicon and even enhance mechanical properties by forming a ceramic matrix. However, the final microstructure of presintered composites (RI) is similar to that of RB composites (preforms are infiltrated only after compacting), with the same amount of residual silicon. It appears that liquid silicon attacks the boundaries between B_4C particles within partly sintered performs and transforms these boundaries to rim regions consisting of the ternary $B_{12}(B,C,Si)_3$ carbide phase.[19] In the case of RB composites, B_4C particles are interconnected by the same ternary $B_{12}(B,C,Si)_3$ carbide phase. Thus, rim regions connect the original B_4C particles in both types of composites, which, independently of the presence of preliminary sintering, display similar microstructures and phase compositions, leading to similar mechanical properties. Therefore, this presintering processing step is useless.

Another important parameter that dictates the best processing approach for RBBC composites is the reliability of products. Using the Weibull approach,[20] RI and RB materials exhibit the same Weibull modulus value ($m \approx 5.6$), whereas this value is significantly lower for RIC ($m \approx 3.14$). RBM composites have a fantastic Weibull modulus value ($m \approx 13.3$), which we attribute to the high level of homogeneity of this composite.

Finally, the use of RBBC composites for light-armor applications has expanded dramatically in the past two decades. Those original works, ongoing for more than 20 years, set the path for improvements in RBBC technology. Ballistic efficiency according to depth of penetration (DOP) tests shows remarkable improvements in RBBC materials. Twenty years ago, RBBC composites had ballistic weight efficiencies (measure of stopping power relative to weight, in which a higher value indicates better performance) that were little higher than those of Al_2O_3. Today, RBM materials reach a ballistic efficiency close to that of hot-pressed B_4C. This patented strategy[21] is now implemented in a new series of armor products made by the PAXIS company in Israel.

Acknowledgments

Shmuel Hayun expresses deep appreciation to Nahum Frage, Moshe P. Dariel, and Eugene Zaretsky for more than 15 years of joint research and valuable discussions in this area.

About the author

Shmuel Hayun is with the Department of Materials Engineering at Ben-Gurion University of the Negev (Beer-Sheva, Israel). Contact Hayun at hayuns@bgu.ac.il.

References

[1]J.C. LaSalvia, J. Campbell, J. Swab, and J. McCauley, "Beyond hardness: Ceramics and ceramic-based composites for protection," *JOM*, **62** [1] 16–23 (2010).

[2]A. Krell and E. Strassburger, "Separation and hierarchic order of key influences on the ballistic strength of opaque and transparent ceramic armor"; pp. 1053–64 in *Proceedings of 27th International Symposium on Ballistics* (Freiburg, Germany, April 22–26, 2013). DEStech Publications, Lancaster, Pa., 2013.

[3]P. Popper, "The preparation of dense self-bonded silicon carbide," *Spec. Ceram.*, 209–19 (1960).

[4]Y.M. Chiang, R.P. Messner, C.D. Terwilliger, and D.R. Behrendt, "Reaction-formed silicon carbide," *Mater. Sci. Eng. A*, **A144**, 63–74 (1991).

[5]J.N. Ness and T.F. Page, "Some factors affecting mechanical and microstructural anisotropy in reaction-bonded silicon carbides"; pp. 347–65 in *Tailoring Multiphase and Composite Ceramics: Proceedings of the Twenty-First University Conference on Ceramic Science*. Plenum Press, New York, 1986.

[6]M.K. Aghajanian, B.N. Morgan, J.R. Singh, J. Mears, and R.A. Wolffe, "A new family of reaction-bonded ceramics for armor applications"; pp. 527–39 in Ceramic Transactions, Vol. 134, *Ceramic Armor Material by Design*. Edited by J.W. McCauley and A. Crowson. American Ceramic Society, Westerville, Ohio, 2001.

[7]J.N. Ness and T.F. Page, "The structure and properties of interfaces in reaction-bonded silicon carbides"; in *Tailoring Multiphase Composite Ceramics*, 1986.

[8]M.S. Naylor and T.F. Page, "Microstructural studies of the temperature-dependence of deformation structures around hardness indentations in ceramics," *J. Microsc.*, **130**, 345–60 (1983).

[9]K.M. Taylor and R.J. Palicka, "Dense carbide composite for armor and abrasives," U.S. Pat. No. 3 765 300, 1973.

[10]M.K. Aghajanian, A.L. McCormick, B.N. Morgan, and A.F. Liszkiewicz Jr., "Boron carbide composite bodies, and methods for making same," U.S. Pat. No. 7 332 221, 2008.

[11]S. Hayun, H. Dilman, M.P. Dariel, N. Frage, and S. Dub, "The effect of carbon source on the microstructure and the mechanical properties of reaction-bonded boron carbide"; 29527–3939 in Ceramic Transactions, Vol. 209, *Advances in Sintering Science and Tevhnology*. Edited by E. A. Olevsky and R. Bordia. Wiley, New York, 2010.

[12]S. Hayun, A. Weizmann, M.P. Dariel, and N. Frage, "Microstructural evolution during the infiltration of boron carbide with molten silicon," *J. Eur. Ceram. Soc.*, **30** [4] 1007527–3914 (2010).

[13]R. Pampuch, J. Bialoskorski, and E. Walasek, "Mechanism of reactions in the Si_L + C_F system and the self-propagating high-temperature synthesis of silicon carbide," *Ceram. Int.*, **13** [1] 63–68 (1987).

[14]J.N. Ness and T.F. Page, "Microstructural evolution in reaction-bonded silicon carbide," *J. Mater. Sci.*, **21** [4] 1377–97 (1986).

[15]A. Favre, H. Fuzellier, and J. Suptil, "An original way to investigate the siliconizing of carbon materials," *Ceram. Int.*, **29** [3] 235–43 (2003).

[16]S. Hayun, A. Weizmann, M.P. Dariel, and N. Frage, "The effect of particle size distribution on the microstructure and the mechanical properties of boron carbide-based reaction-bonded composites," *Int. J. Appl. Ceram. Tec.*, **6** [4] 492–500 (2009).

[17]S. Hayun, M.P. Dariel, N. Frage, and E. Zaretsky, "The high-strain-rate dynamic response of boron carbide-based composites: The effect of microstructure," *Acta Mater.*, **58** [5] 1721–31 (2010).

[18]S.K. Lee, Y.C. Kim, and C.H. Kim, "Microstructural development and mechanical properties of pressureless-sintered SiC with plate-like grains using Al_2O_3–Y_2O_3 additives," *J. Mater. Sci.*, **29** [20] 5321–26 (1994).

[19]S. Hayun, N. Frage, and M.P. Dariel, "The morphology of ceramic phases in B_xC–SiC–Si infiltrated composites," *J. Solid State Chem.*, **179** [9] 2875–79 (2006).

[20]W. Weibull, "A statistical distribution function of wide applicability," *J. Appl. Mech.*, **18**, 293–97 (1951).

[21]S. Hayun, M. Dariel, A. Weizman, and N. Frage. "Process for manufacturing a composite based on boron carbide," Israel (IL) Pat. No. 188517, 2007. ■